NOAA Technical Memorandum OAR PMEL-130

KEO Mooring Engineering Analysis

Noah Lawrence-Slavas, Christian Meinig, and Hugh Milburn

Pacific Marine Environmental Laboratory
7600 Sand Point Way NE
Seattle, WA 98115-6349

June 2006

Contribution 2930 from NOAA/Pacific Marine Environmental Laboratory

NOTICE

Mention of a commercial company or product does not constitute an endorsement by NOAA/OAR. Use of information from this publication concerning proprietary products or the tests of such products for publicity or advertising purposes is not authorized.

Contribution No. 2930 from NOAA/Pacific Marine Environmental Laboratory

For sale by the National Technical Information Service, 5285 Port Royal Road
Springfield, VA 22161

Contents

1. Introduction 1
1.1 Mooring History 1
1.2 Mooring Design 5
1.2.1 2004 (Initial) Deployment 5
1.2.2 2005 Buoy Turn-Around 6
2. Environmental Conditions and Load Cell Data Leading to Failure 7
2.1 Environmental Conditions 7
2.2 2005 Load Cell Post calibration 8
3. Mooring Failure Analysis 8
3.1 Line Failure 8
3.2 Mooring Wear Analysis 11
3.3 Shock Loading Analysis 11
4. WHOI CABLE Analysis 17
4.1 Initial Mooring Analysis 17
4.2 Post Failure Mooring Analysis 18
5. Conclusions 25
5.1 Line Failure 25
5.2 2006 KEO Mooring Design 27
6. Acknowledgments 29

List of Figures

1 Kess observing array. 2
2 Buoy positions. 2
3 2004 mooring configuration. 3
4 2005 mooring configuration. 4
5 NOAA PMEL $^3/_8''$ jacketed wire rope fairing. 5
6 2005 KEO buoy. 7
7 KEO site current profiles. 8
8 Physical conditions for the 6 months leading to failure. 9
9 Physical conditions for the week prior to failure. 10
10 Pre and post-2005 deployment load cell calibration curve. 11
11 $^3/_4''$ 8-strand plaited nylon: section A change in pik length. 12
12 $^3/_4''$ 8-strand plaited nylon line structure in vicinity of break. 13
13 $^3/_4''$ 8-strand plaited nylon: section C pik detail. 14
14 $^3/_4''$ 8-strand plaited nylon: section C kink. 14
15 $^3/_4''$ 8-strand plaited nylon: section F (top view). 15
16 $^3/_4''$ 8-strand plaited nylon: section F (bottom view). 15
17 $^3/_4''$ 8-strand plaited nylon: section F–G parted end. 16
18 $^3/_4''$ 8-strand plaited nylon: section G parted end. 16
19 $^3/_4''$ 8-strand plaited nylon: KEO recovered nylon cut fiber patch. . . 17
20 Clevis wear between the 2004 deployment and the 2005 deployment. 17
21 Archived WW3 satellite wave data for wave heights. 18
22 CABLE static line tension vs. water depth, 2004 deployment. 19
23a Physical conditions for 6 days bracketing 2005156190000. 21
23b CABLE dynamic line tension vs. time for 2005156190000. 21
24a Physical conditions for 6 days bracketing 2005187190000. 22

24b CABLE dynamic line tension vs. time for 2005187190000. 22
25a Physical conditions for 6 days bracketing 2005197130000. 23
25b CABLE dynamic line tension vs. time for 2005197130000. 23
26a Physical conditions for 6 days bracketing 2005285070000. 24
26b CABLE dynamic line tension vs. time for 2005285070000. 24
27 CABLE dynamic line tension vs. time for the week preceding failure. 25
28 Damage to $^3/_8''$ jacketed wire rope at a depth of ∼547 m. 26
29 Damage to $^3/_8''$ jacketed wire rope at a depth of ∼547 m. 26
30 TAO $^3/_4''$ 8-strand plaited nylon: pic length change (E927). 26
31 WHOI CABLE dynamic line tension vs. time, 2006 deployment vs. 2005 deployment. 27
32 WHOI cable dynamic line tension vs. time, 2006 deployment, for mean currents, max currents, and max currents +30% 28
33 KEO 2006 deployment mooring profile during max currents. 28
34 KEO 2006, mooring configuration. 30

KEO Mooring Engineering Analysis

Noah Lawrence-Slavas, Christian Meinig, and Hugh Milburn

Abstract. As a contribution to the global network of OceanSITES time series reference sites a Kuroshio Extension Observatory (KEO) mooring was deployed by NOAA/PMEL in the recirculation gyre in June 2004. The low-cost KEO mooring includes a suite of meteorological, chemical, subsurface, and engineering instrumentation reporting in real time. The mooring was designed to withstand the strong and deep western ocean boundary currents, and the harsh surface conditions found in the Kuroshio Extension region. The observatory returned near 100% data return for 18 months, providing an important data set in an area that is sparsely sampled and has the largest air-sea fluxes in the Pacific. On 6 November 2005, in relatively benign conditions, the KEO buoy broke loose from its mooring and fortuitously was recovered 2 days later. Post failure inspection of the mooring line revealed the mooring had parted in the middle of a continuous section of $^3/_4''$ nylon, 300 m below the lower terminus of the jacketed wire rope, ∼1000 m below the surface. Additionally, analysis of the load cell data exposed concerning patterns of shock loading throughout the deployment period. This report focuses on the KEO mooring design and failure analysis. The wealth of environmental and engineering data available for this mooring gave PMEL engineers a rare opportunity to compare model results with actual observations.

1. Introduction

1.1 Mooring History

The KEO (Kuroshio Extension recirculation gyre Observatory, `www.pmel.noaa.gov/keo`) buoy was deployed by PMEL in the North Pacific Ocean, southeast of Yokohama, Japan in 5685 m of water on 16 June 2004 at 32°21.0′N, 144° 38.2′E (see Fig. 1). The buoy and upper 700 m of mooring were replaced in May 2005 (see Figs. 3 and 4). The KEO mooring is a modified TAO mooring, designed for the harsh conditions of the Kuroshio Extension region (see Fig. 3 (2004) and Fig. 4 (2005)). Modifications include:

- Slack line reverse catenary mooring design, with scope (mooring line/ water depth) of 1.4
- Sonic anemometer
- Modifications to the buoy platform and mooring line for added buoyancy and reduced drag
- 3100 kg anchor

The KEO mooring carries a suite of meteorological sensors to measure pCO_2, winds, air temperature, relative humidity, rainfall, and solar and longwave radiation. Additionally, the KEO mooring carries surface and subsurface instrumentation for measuring temperature and salinity and currents from 1 m to 500 m, and a load cell located at the upper terminus of the mooring, between the buoy bridle and inductive cable. Sensor information is transmitted back to PMEL in "near real time" using satellite communications.

The KEO buoy, sensors, and the upper 700 m (inductive cable) of the mooring were replaced on 28 May 2005 as part of the regularly scheduled

maintenance cycle. PMEL's pCO_2 (air-sea CO_2 flux) measurement system was added to the instrumentation suite during this platform swap, three Sontek current sensors were added to the inductive cable, 17 additional temperature/salinity modules, and a 2nd-generation load cell (IPS V918) replaced the 1st-generation load cell on the original mooring. The 1st-generation load cell (IPS1/V910) recovered during the May swap had failed after ~6 months, when the data cable connecting the load cell to the CPU package failed due to bending fatigue acting on a small section of unsupported cable. Additionally, post deployment calibration showed that the 1st-generation load

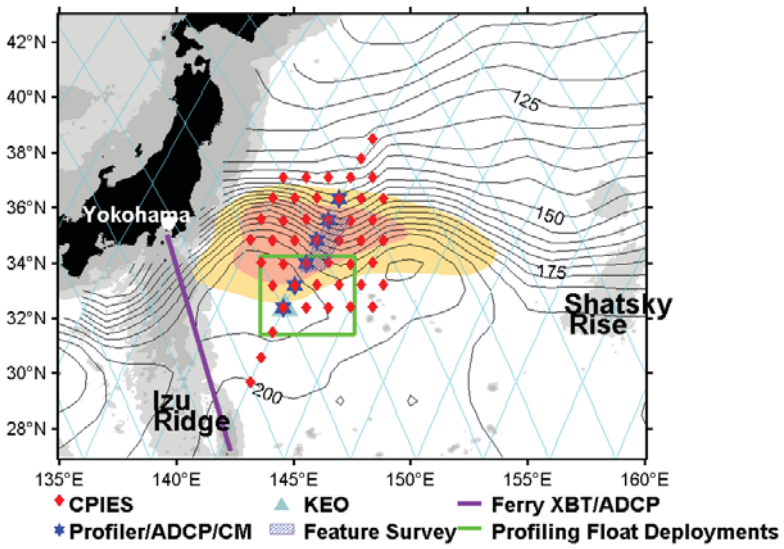

Figure 1: Kess observing array.

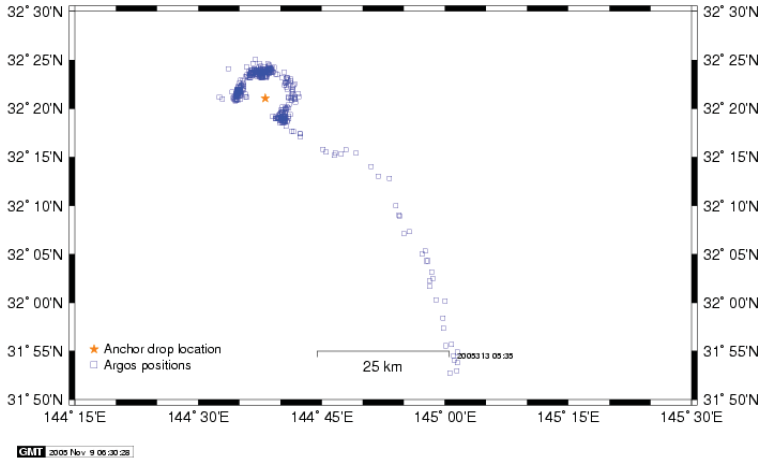

Figure 2: Buoy positions.

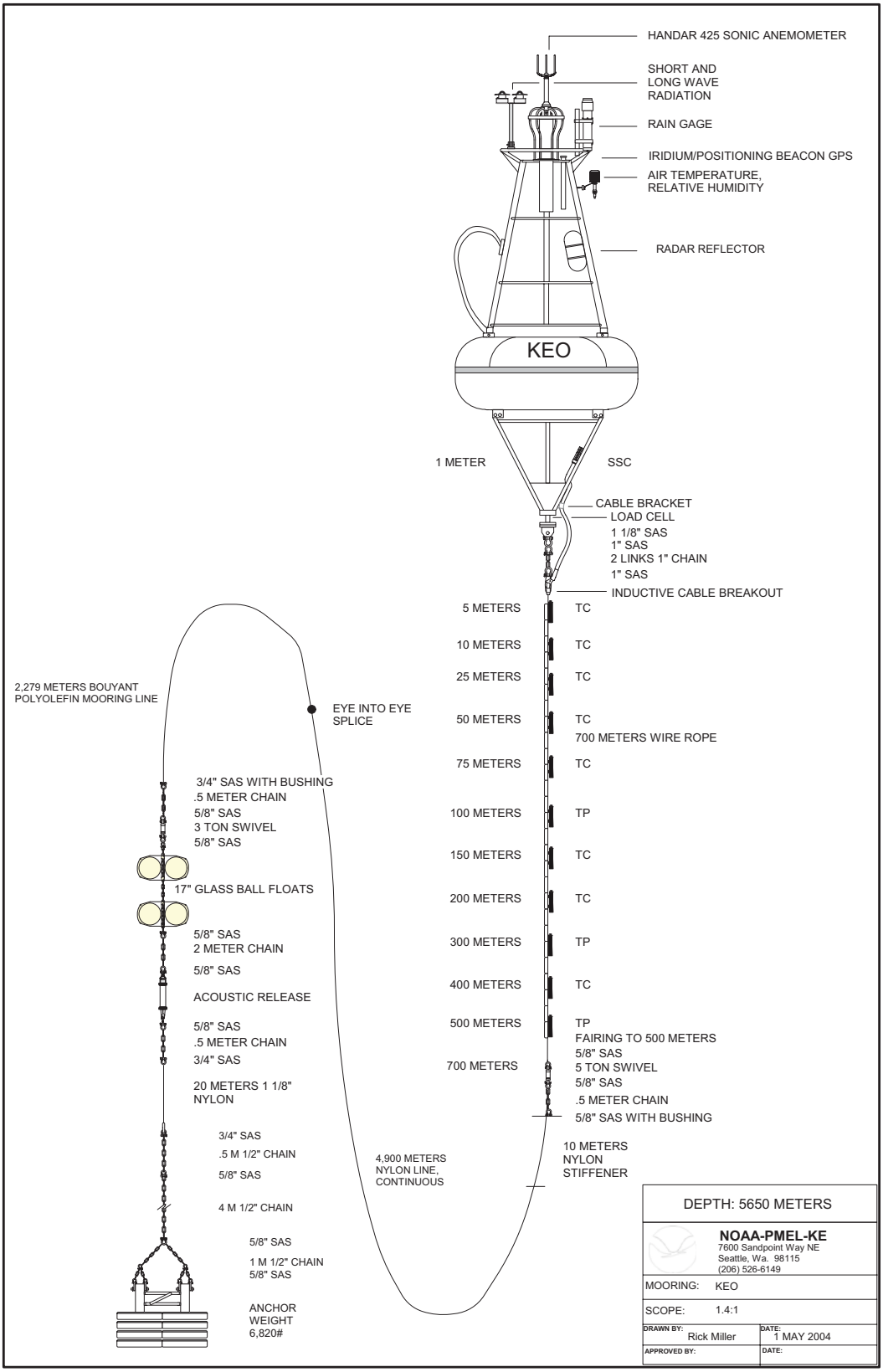

Figure 3: 2004 mooring configuration.

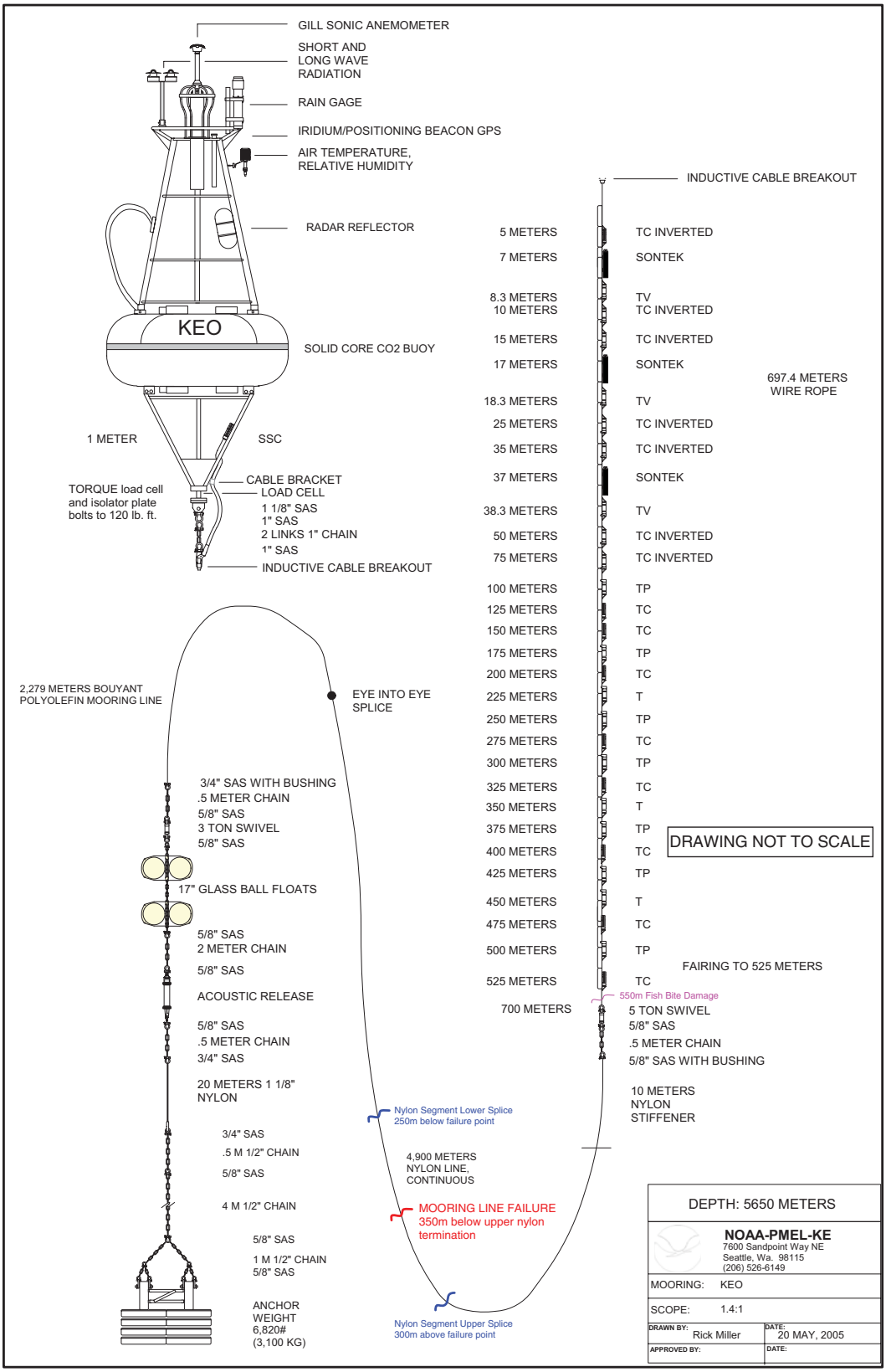

Figure 4: 2005 mooring configuration.

cell had "drifted" during deployment, and that all of the recovered load cell data was corrupt. The 2nd-generation load cell addresses the issues with the 1st-generation load cell, including replacing the 1st generation's voltage output with a current output.

On 12 October 2005 the pCO_2 system ceased transmitting (see pCO_2 KEO Failure.doc), and at ∼1510Z 6 November 2005 position data indicated that the KEO mooring had gone adrift (see Fig. 2). Before the pCO_2 system ceased transmitting, the lab was receiving GPS position data on the KEO mooring every 3 hours. After the pCO_2 system failed, GPS position data was received every 3 days via the IPS-load cell instrument, and 11 times per day via Argos.

The buoy, 700 m of inductive cable, 350 m of nylon mooring line, and all instruments were recovered by the RV *Kaiyo* on 8 November 2005, only 2 days after the mooring went adrift. The recovered mooring was then transported fully assembled to Japan, where it was carefully broken down by a PMEL mooring technician, packaged, and shipped back to Seattle, Washington.

1.2 Mooring Design

1.2.1 2004 (Initial) Deployment

The KEO mooring was designed as a slack line reverse catenary mooring. The mooring was designed to have a scope of 1.4 to survive in harsh current regimes, and the reverse catenary design keeps the upper segment of the mooring fairly vertical. The mooring is composed of the following segments (top to bottom):

1. The KEO buoy is a 2.3 m ATLAS toroid with the center "donut" hole glassed over and filled with foam. The gross displacement of the buoy is ∼5600 lbs, and the net positive displacement of the entire mooring system is ∼5040 lbs.

2. Non-rotating $\frac{3}{8}''$ (0.92 cm) diameter wire rope jacketed to $\frac{1}{2}''$ (1.27 cm) is used in the upper 700 m to guard against damage from fish bite, and to form the inductive loop. The upper 500 m of this cable are faired with PMEL's extruded plastic snap on fairings (see Fig. 5). The fairing design is based on a standard airfoil shape with a t/c (width/length) around 0.25.

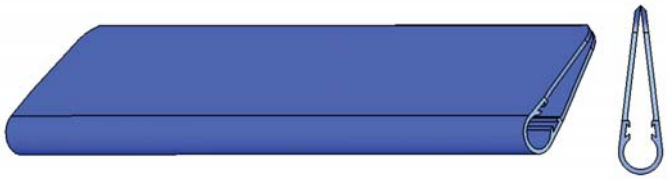

Figure 5: NOAA PMEL $\frac{3}{8}''$ jacketed wire rope fairing.

3. Plaited 8-strand $^{3}/_{4}''$ ($^{11}/_{16}''$ nom., 1.9 cm) diameter nylon line is used for the next 4900 m of the mooring (composed of ∼550 m line segments "end to end braided short spliced" together). The upper 10 m is coated with polyurethane nylon stiffener.

4. The nylon is then "end to end braided short spliced" to 2280 m of buoyant $^{7}/_{8}''$ polyolefin line.

5. The anchor is fabricated from scrap railroad wheels and weighs ∼3100 kg.

All hardware is standard equipment as used in other PMEL moorings and deployments follow the traditional anchor last routine. Subsurface modules are clamped around the jacketed cable, and are standard TAO instrumentation.

For the 2004 deployment, the mooring was rigged as shown in Fig. 3. The mooring modeling program, WHOI CABLE, was used to evaluate the mooring design prior to the initial deployment.

1.2.2 2005 Buoy Turn-Around

The KEO mooring survived for 18 months before failure. After 12 months the mooring was serviced. Servicing was performed by lifting the buoy out of the water with the ship's crane, and then recovering the 700 m of wire rope with a capstan. The procedure was designed to recover and replace only the buoy and wire rope, not the nylon. Excellent ship handling, centering the ship directly above the anchor using the signal from the acoustic release, and the 1.4:1 scope of the mooring, allowed the recovery to be accomplished, while keeping the load below the SWL of the wire and nylon. Redeployment consisted of substituting a new buoy, a new piece of 700 m of wire and attached instruments, a new swivel and $^{1}/_{2}$ m piece of chain, above the nylon. Additionally the following changes were made (see Fig. 4):

- Added 3 Sontek current sensors to the inductive cable (within the top 37 m of mooring, ∼ neutrally buoyant).

- Added 17 temperature/salinity modules to the inductive cable (+17 lbs. wet weight).

- Added a buoy mounted pCO_2 system (+150 lbs. embedded in buoy ∼12″ above waterline) (see Fig. 6).

- Replaced 1st-generation load cell with 2nd-generation load cell (physical dimensions nearly identical).

2. Environmental Conditions and Load Cell Data Leading to Failure

2.1 Environmental Conditions

The following figures (Figs. 7–8) show the environmental conditions observed at the KEO mooring site for the 6-month period ending in the mooring failure. The load cell data (upper terminus of the mooring, between the buoy bridle and inductive cable) collected during this time is of particular interest.

The KEO mooring was subjected to disturbingly high levels of "shock loading" during the last 6 months of its life. Since the 2004 deployment load cell failed during deployment, it is possible the mooring may have been experiencing shock loading over its entire 18-month life. Shock loading occurs when the tension within a segment of the mooring line drops to zero, causing the line to momentarily go slack. When the tension is re-applied to the line, the slack is rapidly taken in, causing an abrupt increase in line tension. The instances of shock loading can be directly related to periods of high wind at the mooring site (see Fig. 8). A comparison of wave "slopes" (Wave Height/$\frac{1}{2}$ * Wave Period, obtained from WW3 satellite wave maps) at the mooring site during these periods of high shock loading is shown in Figs. 8 and 9. Additionally, Fig. 9 shows the loads and conditions seen by the

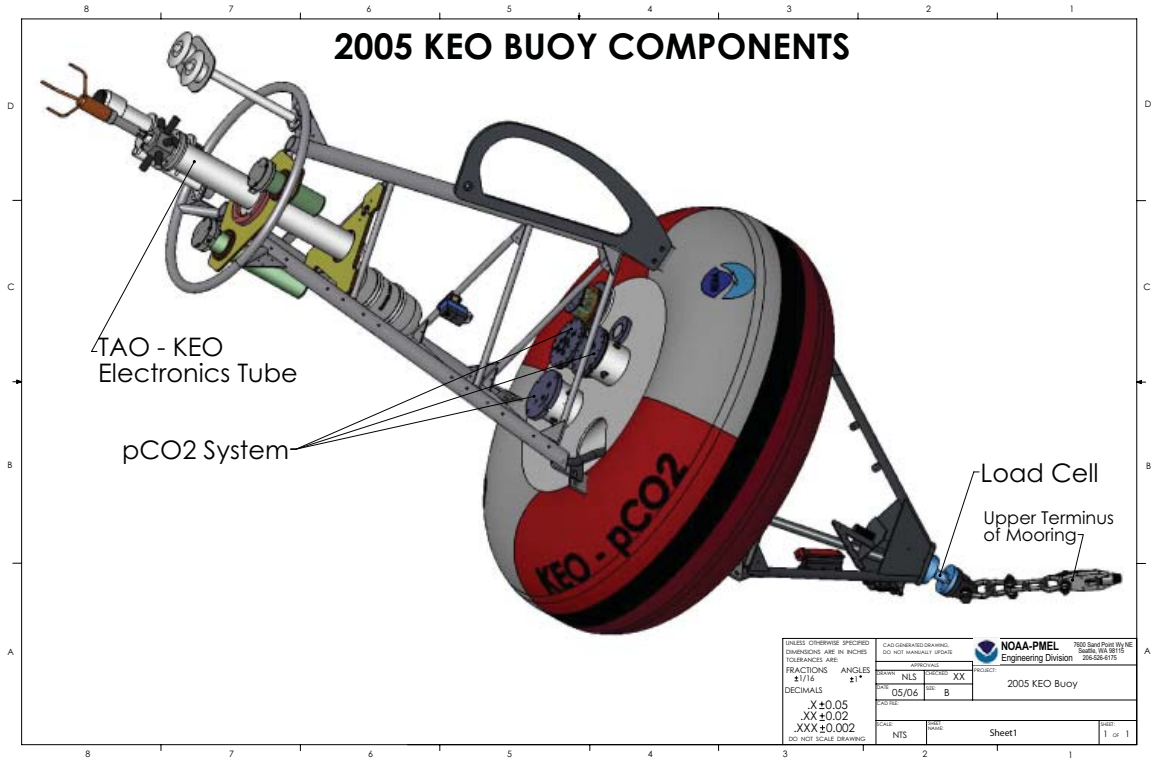

Figure 6: 2005 KEO buoy.

mooring during the week prior to failure. The red dots labeled "interpolated wind with load $\leq$200 lbs" correspond to the times at which the minimum mooring line tension fell below 200 lbs.

2.2 2005 Load Cell Post calibration

Upon recovery, a post calibration routine was run on the load cell. Comparing this post-calibration to the pre-deployment calibration showed that sometime during the KEO deployment the load cell drifted ~75 lbs. in the positive (heavy) direction (see Fig. 10). After consideration, it was determined that this drift could be attributed to errors in the calibration process, and that a 75-lb. error would be lost in the "noise" during deployment and considered insignificant to the overall load cell results.

3. Mooring Failure Analysis

3.1 Line Failure

The KEO mooring line parted at a point 350 m below the junction between the inductive cable and the plaited 8-strand $^{3}/_{4}''$ ($^{11}/_{16}''$ nom.) nylon line, approximately 1050 m below the surface (see Fig. 4). The mooring line failed approximately in the middle of a 550 m piece of nylon (~300 m below

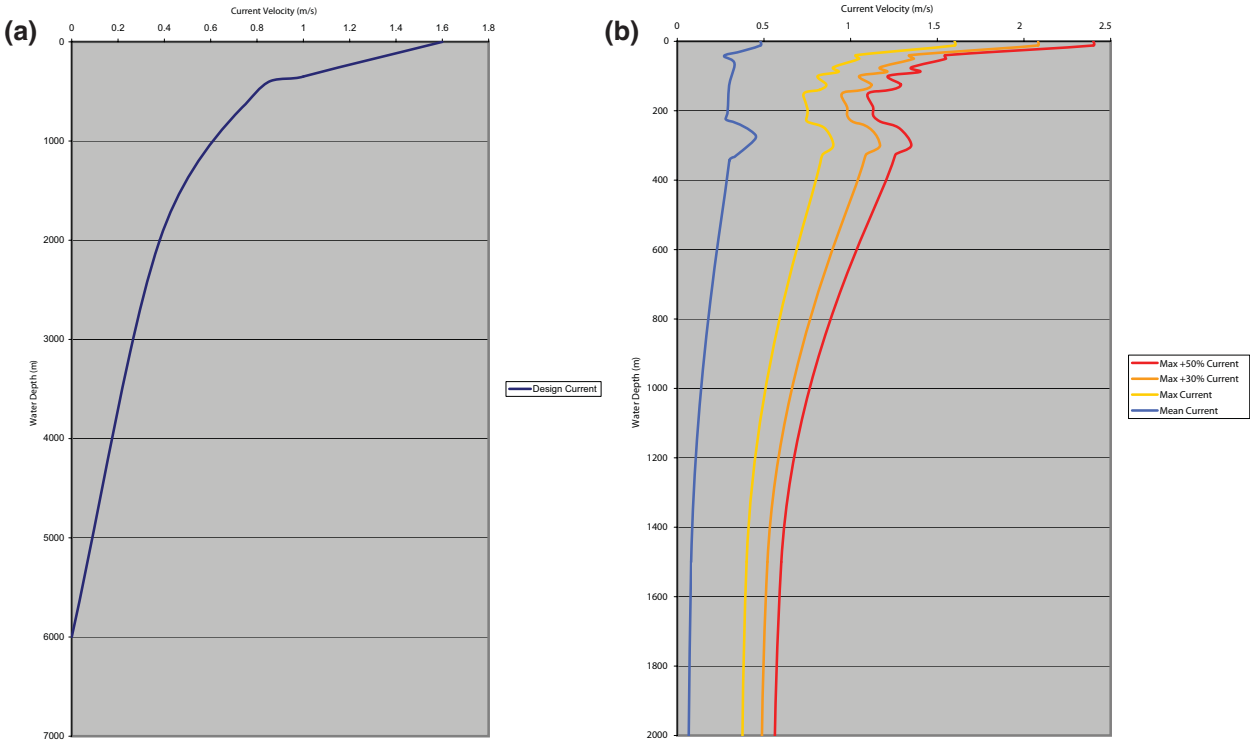

Figure 7: (a) Initial "best guess" current profile, used to design the 2004–2005 KEO mooring. (b) Observed 2005 current profile at KEO site (please note that the current profile is only shown to 2000 m; beyond 2000 m the current remains constant all the way to the bottom at ~5650 m).

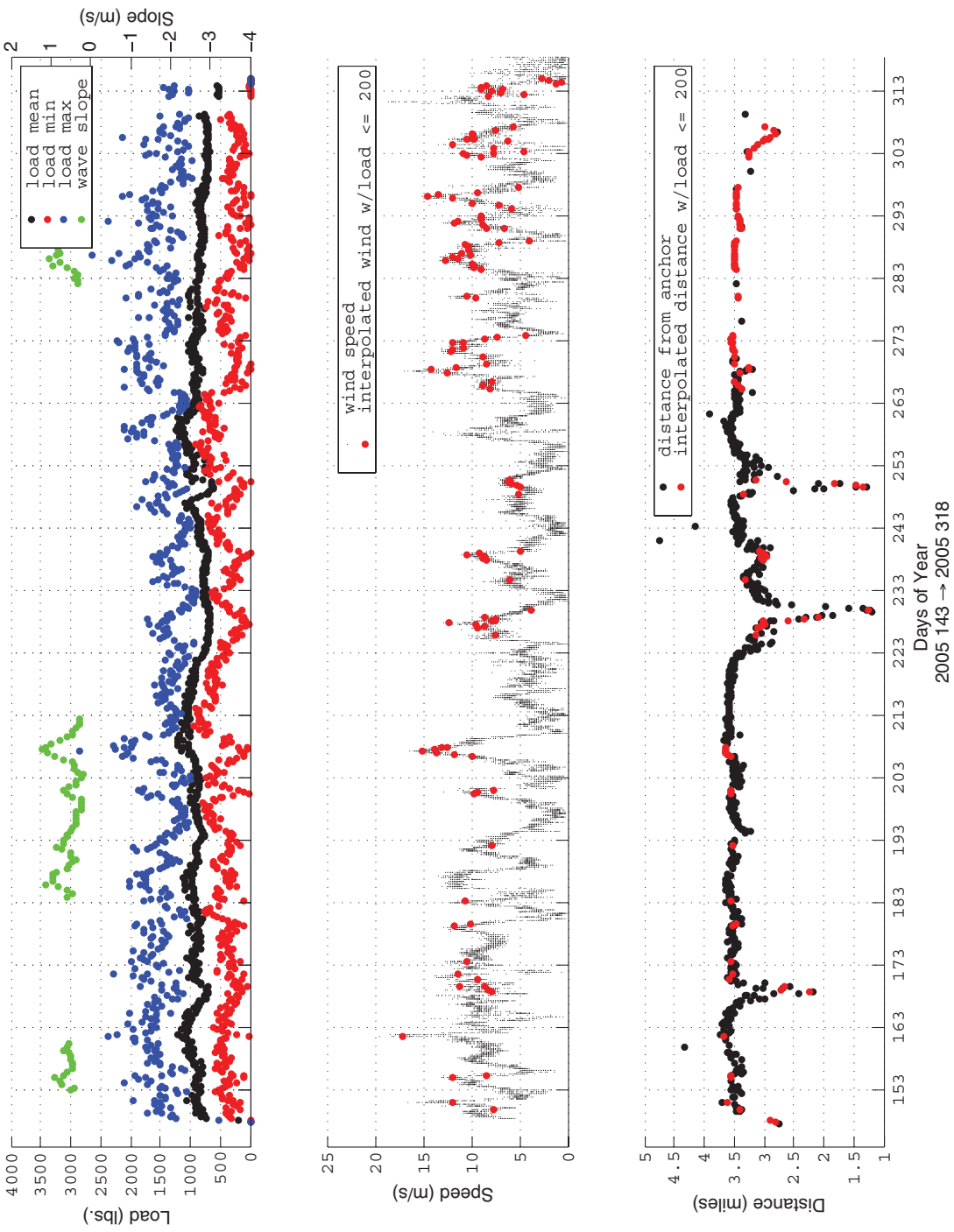

Figure 8: Loads, wave slope, winds, and KEO buoy distance from anchor for the 6 months leading to failure.

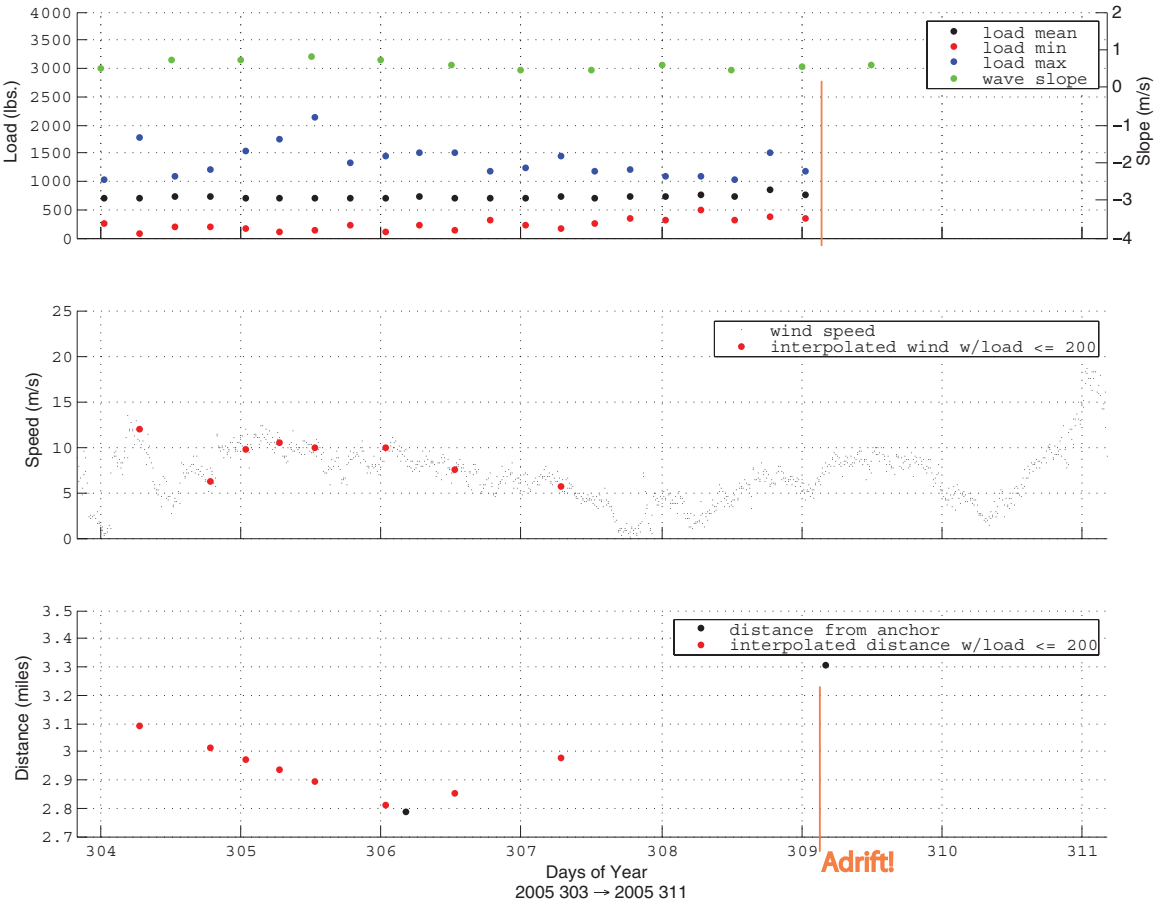

Figure 9: Loads, wave slope, winds, and KEO buoy distance from anchor for the week prior to failure.

the upper line segment splice, and ∼250 m above the lower splice). The recovered inductive cable did show apparent fish bite damage at ∼547 m of water depth (Figs. 28 and 29).

The cause of the line failure is not readily apparent; the unusual mooring line structure in the vicinity of the break is summarized below, and shown in the following figure and photos (Fig. 12).

1. Variable pik lengths of the nylon weave in the segment of line within ∼3.0 m of the break (see Figs. 11, 13, 14, and 17). Visual inspection of the rest of the 350 m of nylon line recovered did not show this structural abnormality in any other location.

2. Strange loops in the line just before the break point that seem to be caused by two strands of the 8-strand line getting hung on each other and missing the weave for 2–3 pik lengths (see Figs. 15 and 16).

3. Kinks in the individual line strands in the areas of the line that have an especially long (∼4″) pik length (see Fig. 14)

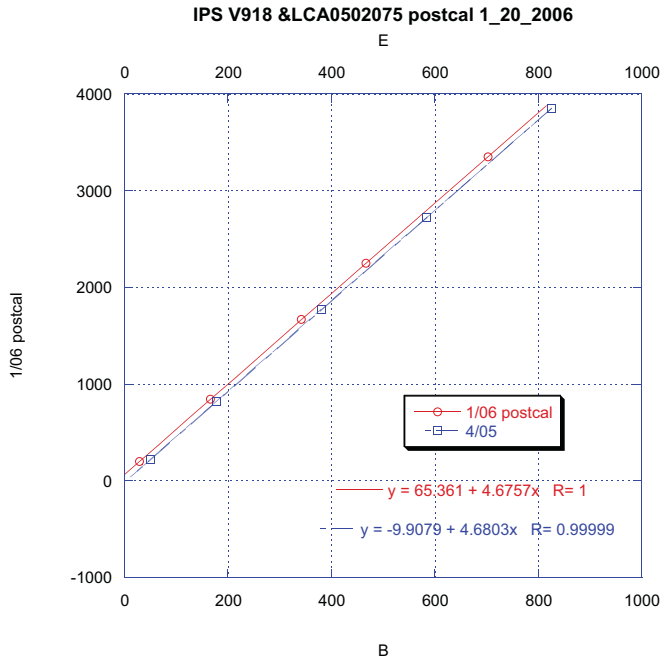

Figure 10: Pre and post-2005 deployment load cell calibration curve.

In addition to the unusual line structure in the vicinity of the break, the rest of the 350 m of recovered line exhibited regularly spaced patches of cut fibers along the outside of the woven strands (see Fig. 19). Studying pictures and notes of the deployment layout failed to yield an explanation for these cut fibers, although the line could have been damaged during recovery operations.

3.2 Mooring Wear Analysis

The clevis is the uppermost terminus of the KEO mooring line, and is hard bolted to the buoy bridle just below the load cell (see Fig. 4). Previous observations indicate that of all the components within the mooring system, the clevis exhibits the highest amount of wear. A comparison of the wear patterns between the initial (12 month) KEO deployment and the second (6 month) deployment showed that the respective clevises exhibited approximately the same amount ($\sim 1/32''$) of wear for both deployments. Since the 2nd deployment's duration was half that of the first deployment, it is assumed that the 2nd deployment's mooring system experienced significantly higher levels of "working" than the initial KEO deployment's mooring (see Fig. 20).

3.3 Shock Loading Analysis

A careful comparison of the KEO load cell data to the wind data, and the WW3 satellite (NOGAPS) wave data (see Fig. 21, and `https://navy.ncdc.noaa.gov/products/products.html`) shows that the KEO mooring begins to experience shock type loading when the wave slope becomes steeper than

~0.70 m/s, and the worst shock loading occurs in wave slopes greater than ~1 m/s (see Fig. 8).

A rough numerical calculation of the terminal vertical velocity of the upper 700 m of the mooring was determined using the following equation:

$$\mathrm{Fdt} = \tfrac{1}{2} * (\mathrm{Cdt}_{\text{flat plate}}) * (\rho) * (\mathrm{A}) * (\mu^2) + \tfrac{1}{2} * (\mathrm{Cdt}_{\text{cable}}) * (\rho) * (\mathrm{A}) * (\mu^2) + \tfrac{1}{2} * (\mathrm{Cdt}_{\text{line}}) * (\rho) * (\mathrm{A}) * (\mu^2)$$

The drag force was assumed to be the weight of the mooring in water, the end effects of the instruments were calculated by assuming the instruments approximated a single flat plate ($\mathrm{Cdt}_{\text{flat plate}} = 1.17$), the tangential drag of the faired cable was calculated using a drag coefficient ($\mathrm{Cdt}_{\text{cable}}$) of 0.03, and the tangential drag coefficient ($\mathrm{Cdt}_{\text{line}}$) of the mooring line was assumed to be 0.003. The $\mathrm{Cdt}_{\text{cable}}$ value of 0.03 was a best guess, "dart throw," 0.03 being a factor of 10 greater then the Cdt of bare cable. The results of this calculation suggested that the instruments and the mooring line contribute relatively little tangential (vertical) drag to the mooring system when compared to the tangential drag of the faired cable, and that the calculated terminal velocity of the upper 700 m of mooring is ~1.10 m/s.

To calculate the mooring's terminal velocity with the wave slope data, it was assumed that the wave slope approximates the vertical rise and fall velocity of the KEO buoy in a given sea state. Therefore it appears that the terminal velocity of the KEO mooring is approximately 0.7 m/s (wave slope at which shock loading begins to occur), not the 1.10 m/s calculated above. This error can probably be attributed to an error in the initial guess for the Cdt of the faired cable (0.03 should be higher), and the fact that in real life the nylon and polyolefin segments of the mooring line are not truly vertical, thus the $\mathrm{Cdt}_{\text{line}}$ of 0.003 that was used for the line drag calculation should be higher. Shock loading occurs when the KEO buoy, traveling down the backside of a wave, falls faster than the mooring line, causing the mooring

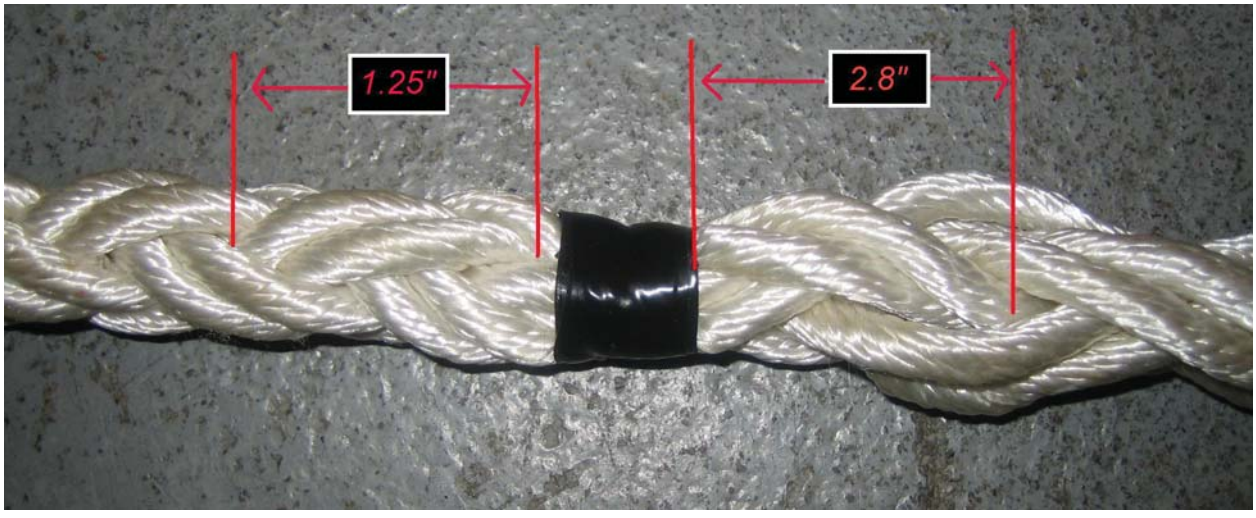

Figure 11: ¾″ 8-strand plaited nylon: section A change in pik length.

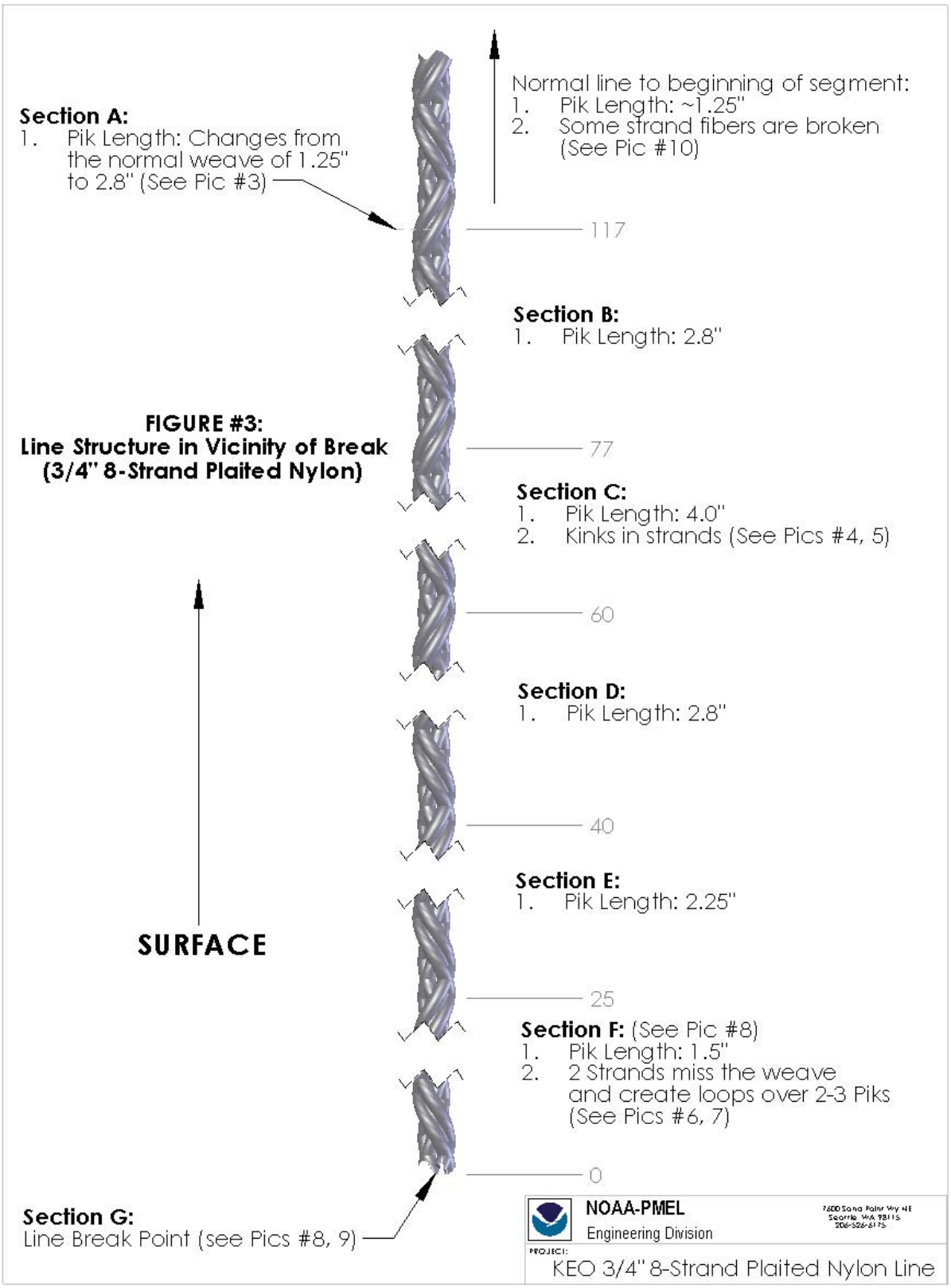

FIGURE #3:
Line Structure in Vicinity of Break
(3/4" 8-Strand Plaited Nylon)

Figure 12: $3/4''$ 8-strand plaited nylon line structure in vicinity of break.

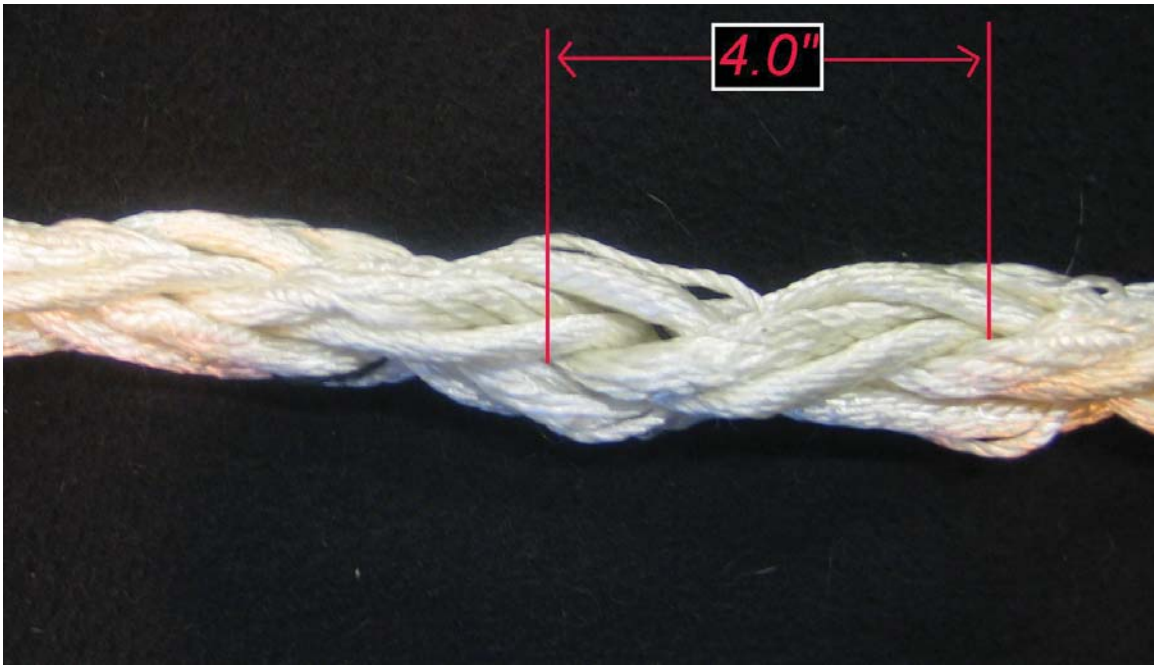

Figure 13: ¾″ 8-strand plaited nylon: section C pik detail.

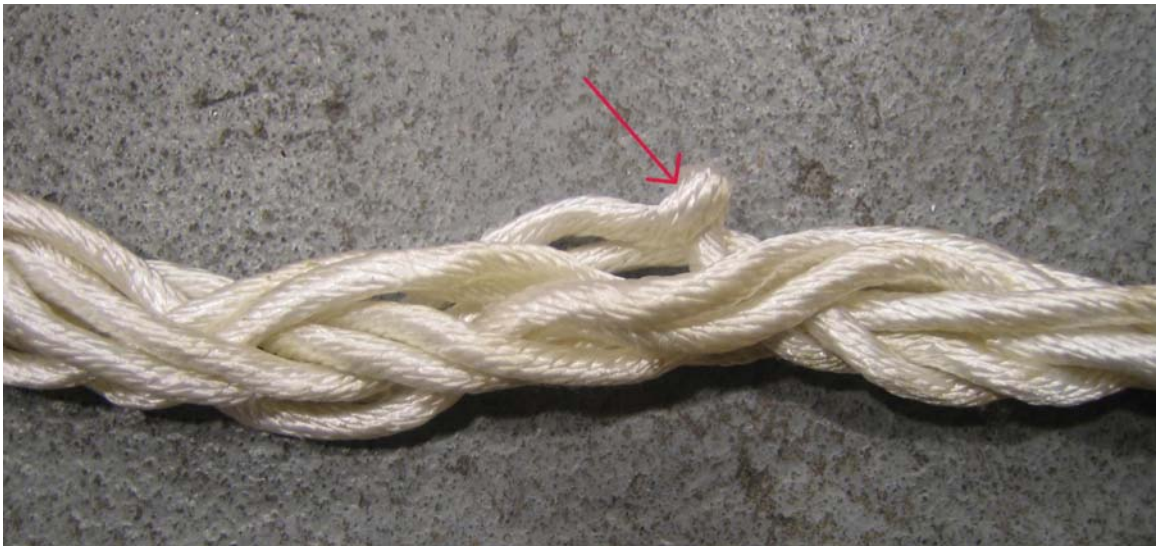

Figure 14: ¾″ 8-strand plaited nylon: section C kink.

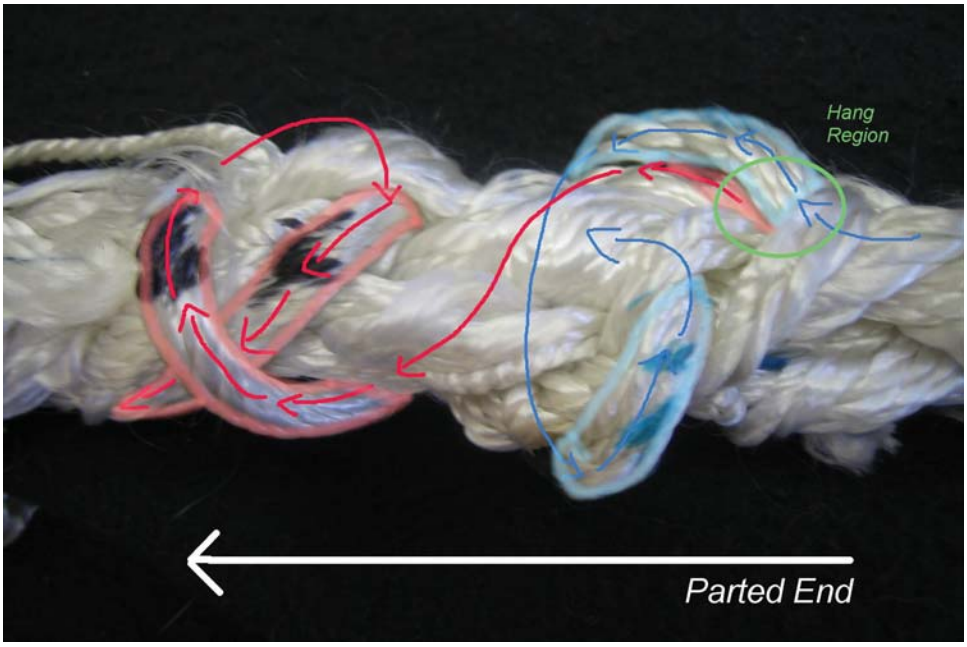

Figure 15: ¾″ 8-strand plaited nylon: section F (top view).

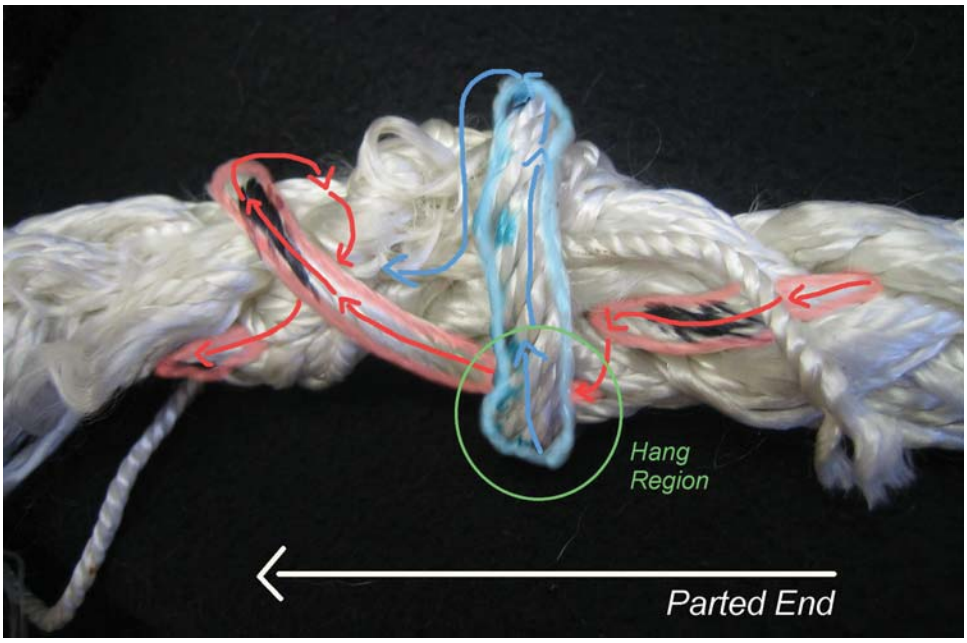

Figure 16: ¾″ 8-strand plaited nylon: section F (bottom view).

Figure 17: ¾″ 8-strand plaited nylon: section F–G parted end.

Figure 18: ¾″ 8-strand plaited nylon: section G parted end.

Figure 19: $^3/_4''$ 8-strand plaited nylon: KEO recovered nylon cut fiber patch.

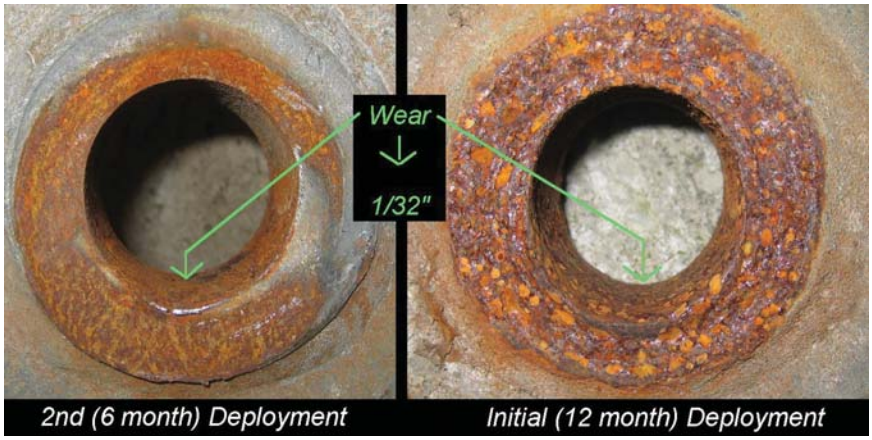

Figure 20: Clevis wear between the 2004 (12-month) deployment and the 2005 (6-month) deployment.

to go momentarily slack. When the buoy begins to climb the face of the next wave this slack is abruptly taken in, causing the shock loading seen in the load cell data. After running many iterations of the KEO mooring in a time domain numerical model, it was determined that the Cdt of the faired cable is ∼0.0501 (see: 4.2, "Post Failure Mooring Analysis").

4. WHOI CABLE Analysis

4.1 Initial Mooring Analysis

Before the initial deployment, the mooring was statically analyzed in WHOI CABLE using a "best guess" current profile (see Fig. 7a), and without the addition of the subsurface instrumentation (see Fig. 22). WHOI CABLE is a time domain numerical simulation of moored and towed oceanographic sys-

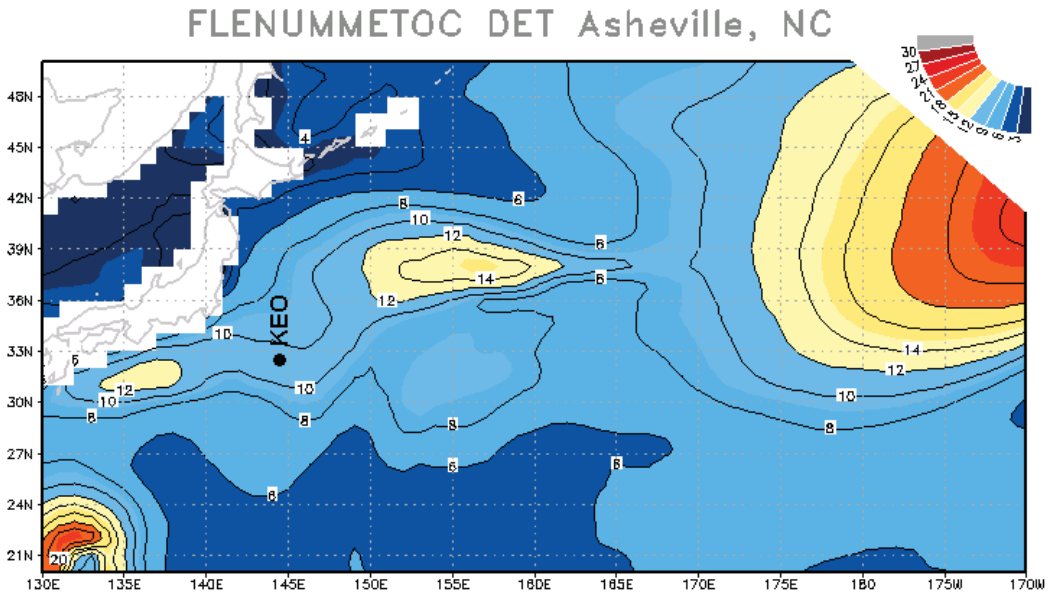

Figure 21: Archived WW3 satellite wave data for wave heights.

tems developed at WHOI. Unfortunately, the load cell deployed during the initial deployment failed, so we were unable to compare the initial CABLE model with measured load data.

4.2 Post Failure Mooring Analysis

After the KEO mooring failed, a concerted effort was made to build an accurate KEO mooring model in WHOI CABLE. During this modeling process all mooring material properties were double checked for accuracy, and the subsurface instruments were modeled as materials and added to the mooring model. Special attention was paid to the faired inductive cable, which was assumed to be the most important unknown variable in the mooring system.

The effects of changing different WHOI CABLE input variables were carefully studied during the model development process. The results of modeling the subsurface instruments as "connectors" vs. "materials" was looked at and found to increase the mooring line tension results in the line above the instruments by ∼6% when using "connectors." The effects of wind forcing upon the model was found to be negligible (>3%) to overall results. Varying the tangential drag coefficient of the faired cable was found to greatly impact the tension "spread" (max-min) of the mooring line, while having a minimal impact on mean mooring tension. Manipulating the wave forcing inputs was also found to impact the mooring tension "spread," although to a lesser extent than the tangential drag coefficient. Varying the normal drag coefficient of the faired cable by a factor of 10, using a current profile of ∼(0, 0.10) (280, 0.83) (500, 0.75) (2000, 0.38) (6000, 0), was found to have only a minimal impact on the mean mooring tension (∼100 lbs.). The current forcing input was found to have significant impact on the mean

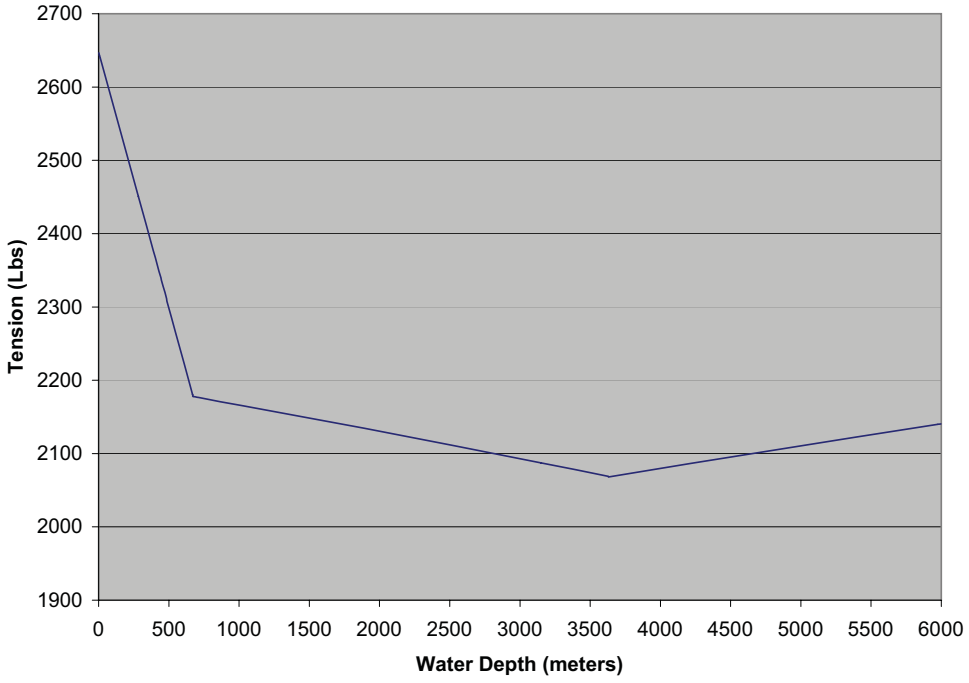

Figure 22: CABLE static line tension vs. water depth, 2004 deployment no instruments.

tension of the mooring, and it is one of the most important forcing inputs in the CABLE model.

In order to attempt to obtain more accurate tangential and normal drag coefficients for the faired cable, a test procedure was developed in which the terminal velocity of the faired inductive cable was obtained experimentally through repetitive vertical and horizontal faired cable drops in the NOAA dive tower. Unfortunately, while this method yielded accurate numbers for the drag on an un-faired cable, the fairings reduced the drag force to such an extent that noise in the data caused by the experimental techniques overwhelmed the drag caused by the faired cable, yielding erroneous results. Equating the observed terminal fall velocity of the mooring to the calculated velocity (see 3.3, "Shock Loading Analysis") yielded a tangential drag coefficient for the faired inductive cable of $\sim$0.108.

Once the KEO mooring was built in CABLE (see: {KEO}{KEO2}{xxxx}{0}.cab), the model was verified for accuracy. This was accomplished by comparing the static mooring tensions, the tension "spread," instrument depths, and the horizontal distances of the buoy from the anchor obtained from the CABLE model during four, distinct, real-life environmental conditions, to the actual load cell data, instrument depth recordings, and buoy positions seen during these environmental conditions. These deployment "snapshots" were picked to cover the range of environmental conditions observed at the deployment site, and special care was taken to eliminate the effects of changing conditions by taking these "snapshots" in the middle of times of relatively stable environmental conditions. The KEO mooring

presented PMEL with a unique post analysis opportunity, due to the large amount of data available on the current profile (primary forcing function) at the buoy site. The complete current profile at the KEO site was collected from WHOI's ADCP profiling buoy array (see Fig. 1). Inputting the mean current profile at the KEO site from 2005 as the primary CABLE forcing function (see Fig. 7b), yielded mean tension results within 60 lbs. for all snapshots except 20051871900. For that snapshot, the mean current profile was adjusted by increasing the current profile by 0.1 m/s to yield accurate tension results. A study of the Navy's current forecast model, NLOM (`http://www7320.nrlssc.navy.mil/global_nlom32/kur.html`), did not yield conclusive evidence as to why snapshot 20051871900 had higher mean tensions than the other periods sampled. However, NLOM did indicate that the mooring site may have encountered a "spin off" current during that time.

The faired inductive cable's normal and tangential drag coefficients were then adjusted (starting at the guess of 0.108, from above) so the CABLE results were in line with the measured results. Since the normal and tangential drag coefficients of circular line are well known, these numbers were not adjusted. The final normal drag coefficient for the faired cable was set at 0.3, and the tangential drag coefficient was set at 0.0501. The "instruments as materials" model was used to mimic the KEO mooring because "materials" more accurately mimic actual bodies in WHOI CABLE dynamic solutions (materials treat drag forces based on shape, not the "approximate sphere" used for connectors). CABLE model results for instrument depth compared to within 2.5% of observed instrument depth (CABLE was always on the deep side), and CABLE results for the horizontal distance from the anchor were within 10% (CABLE always showed the buoy closer to the anchor then observed results). It should be noted that the CABLE results for distance from anchor were almost always ∼10% under, and might be due to a difference in actual deployment depth compared to designed deployment depth. Tension "spread" results were within 8% (∼70 lbs.) of overall tension, as were the mean tension results (∼60 lbs.).

The dynamic results of these mooring models, and the actual conditions observed, are shown below (See Figs. 23–27). The dynamic output of this CABLE file for the time frame in the vicinity of the break is shown in Fig. 27 (see Fig. 9 for observed forces).

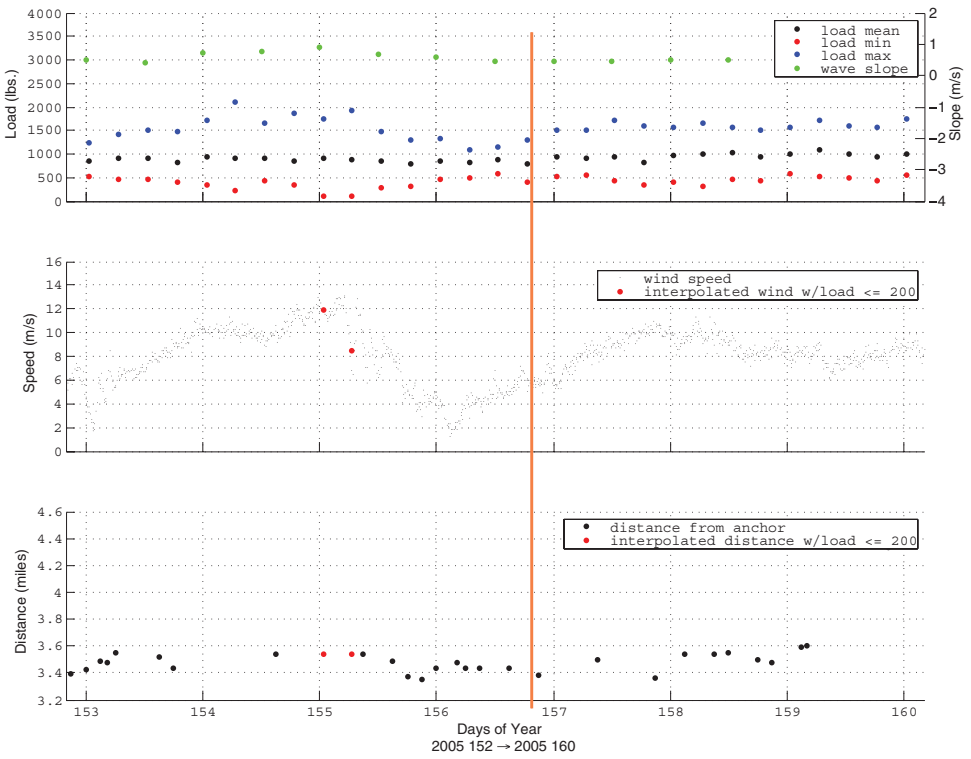

Figure 23a: Loads, wave slope, winds, and KEO buoy distance from anchor for 6 days bracketing 2005156190000.

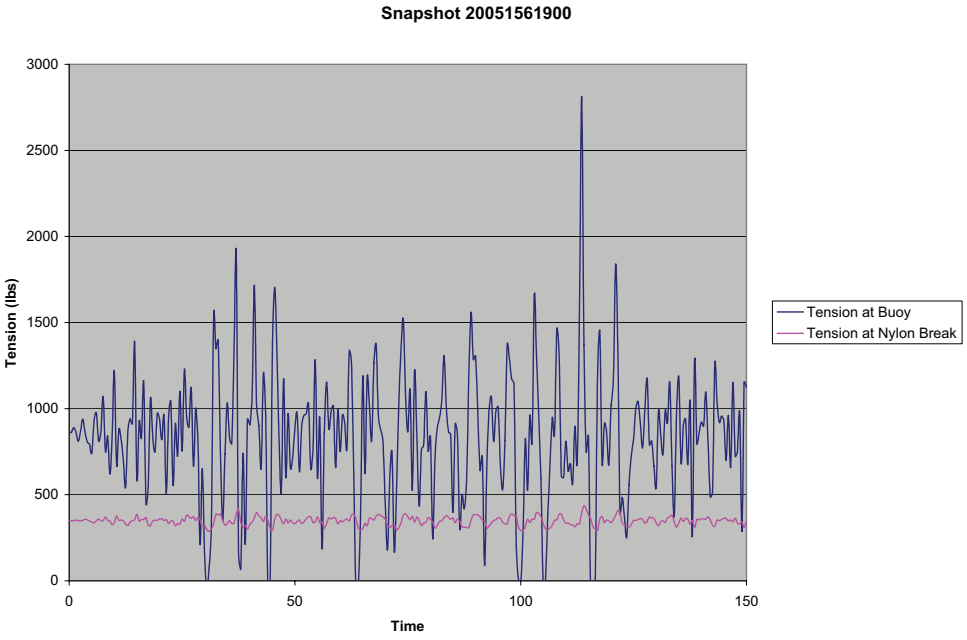

Figure 23b: CABLE dynamic line tension vs. time, 2005 deployment instruments modeled as materials for 2005156190000.

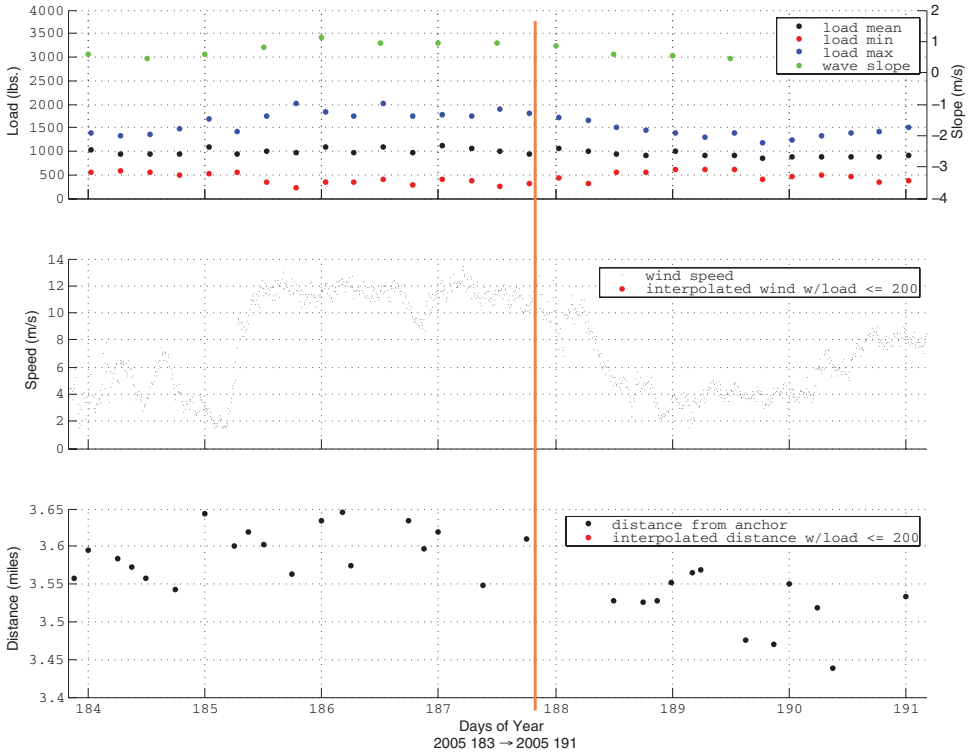

Figure 24a: Wave slope, winds, and KEO buoy distance from anchor for 6 days bracketing 2005187190000.

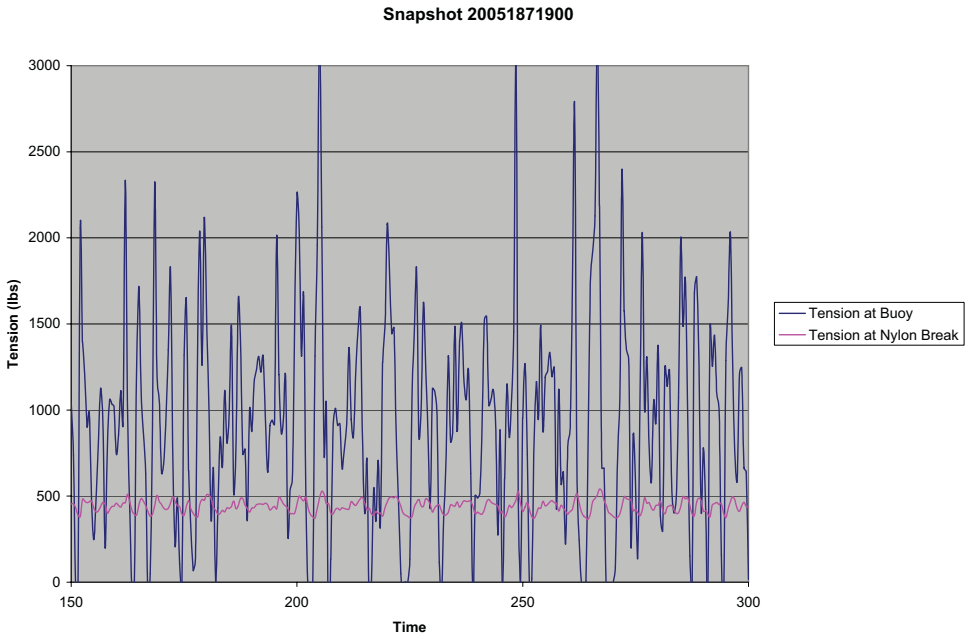

Figure 24b: CABLE dynamic line tension vs. time, 2005 deployment instruments modeled as materials for 2005187190000.

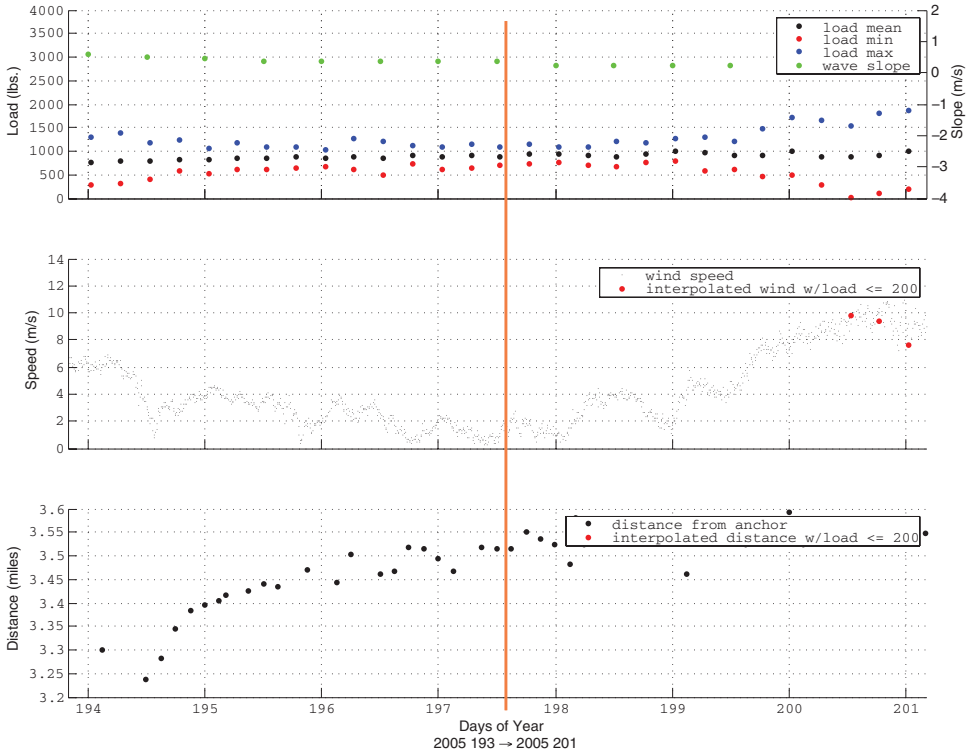

Figure 25a: Wave slope, winds, and KEO buoy distance from anchor for 6 days bracketing 2005197130000.

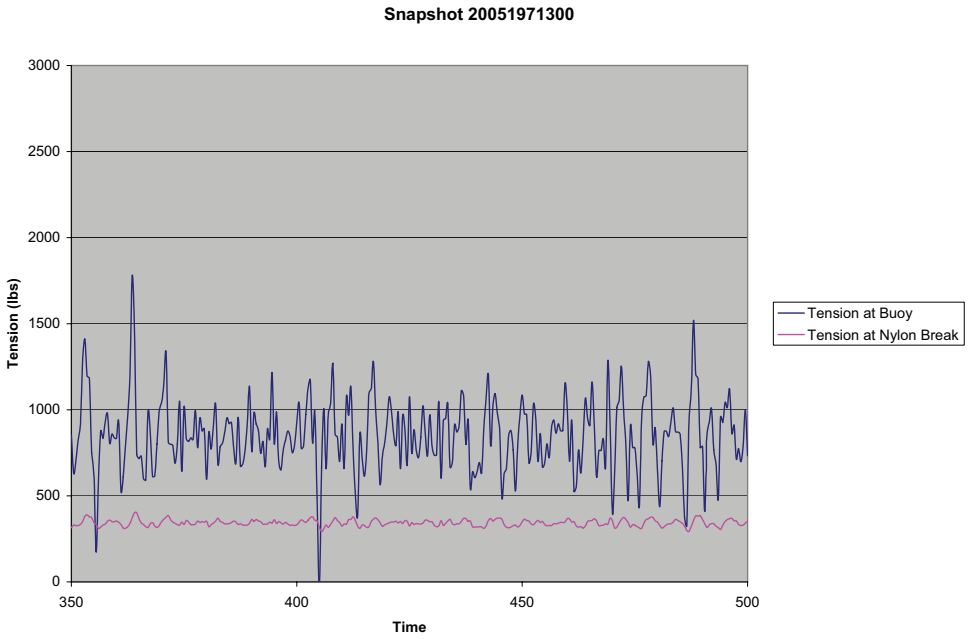

Figure 25b: CABLE dynamic line tension vs. time, 2005 deployment instruments modeled as materials for 2005197130000.

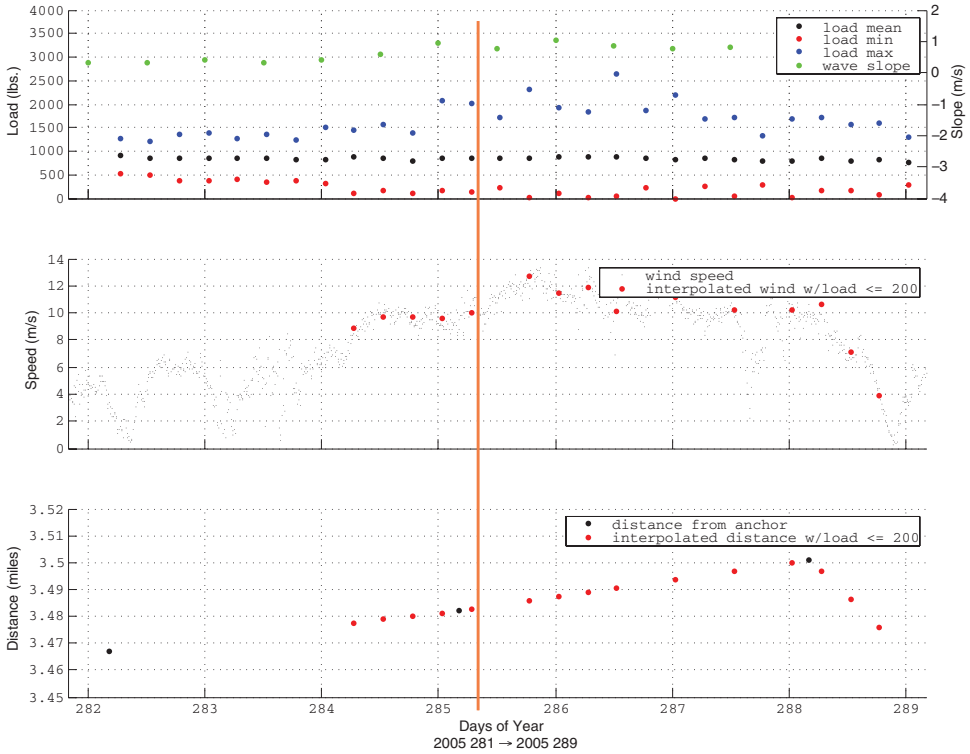

Figure 26a: Wave slope, winds, and KEO buoy distance from anchor for 6 days bracketing 2005285070000.

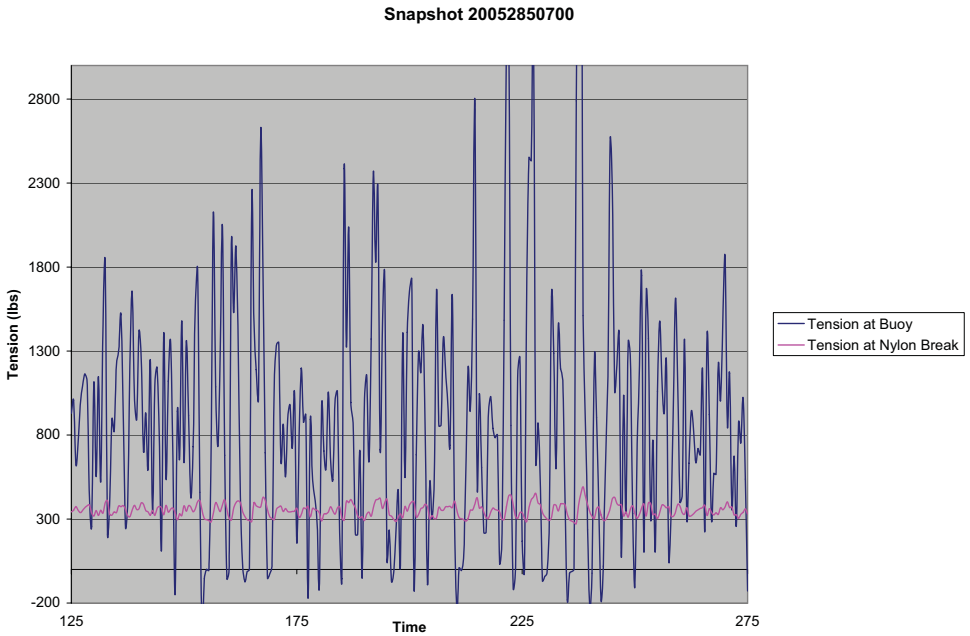

Figure 26b: CABLE dynamic line tension vs. time, 2005 deployment instruments modeled as materials for 2005285070000.

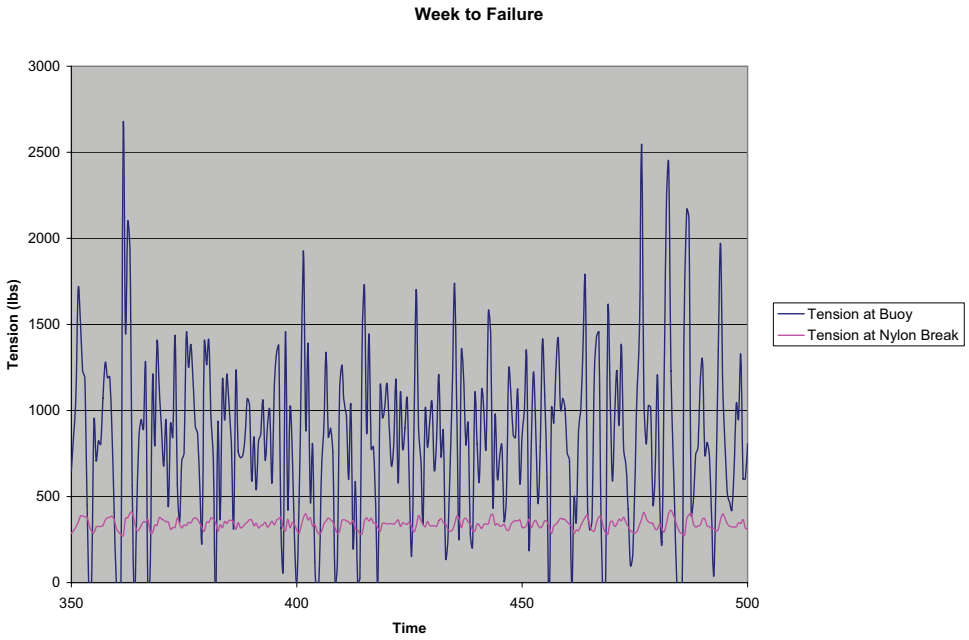

Figure 27: CABLE dynamic line tension vs. time, 2005 deployment instruments modeled as materials for the week preceding failure. Note the many instances of zero tension.

5. Conclusions

5.1 Line Failure

The cause of the line failure is still unknown. Discussions with the rope manufacturer on the baffling line structure in the vicinity of the break have yielded inconclusive results. It is believed that at some point during the deployment some ($\sim$1/5) of the outer strand fibers line were cut and this, combined with the strange line structure, and shock loading eventually resulted in line failure. The strange cuts to the outside of the rope fibers (see Fig. 19) could have been a result of deployment/recovery operations, or damage due to fishing gear. Fish bite at the depth of the break location, $\sim$1000 m, seems unlikely, however we did see heavy fish bite damage to the inductive cable at $\sim$547 m (see Figs. 28 and 29). It is still a mystery as to why the line pik lengths varied so substantially (300%) in the vicinity of the break, why there were the strange braiding problems at the point of failure, and why even with these cut fibers the line failed under such low loads. It is important to note that this change in pik length was also recently observed (to a much less extreme extent) in a small (0.25 m) segment of nylon line recovered off of a taught line TAO buoy moored at 0°, 125°W (see Fig. 30). The TAO line was also 3/4″ 8-strand plaited nylon. However, the TAO line was in no way related to the KEO line, having been made by a different manufacturer.

Segments from both of these recovered lines were tested to determine if the pik length could have been caused during the line stretching and measurement operations. Tests proved that stretching the line to 3500 lbs. and

Figure 28: Damage to 3/8″ jacketed wire rope at a depth of ∼547 m.

Figure 29: Damage to 3/8″ jacketed wire rope at a depth of ∼547 m.

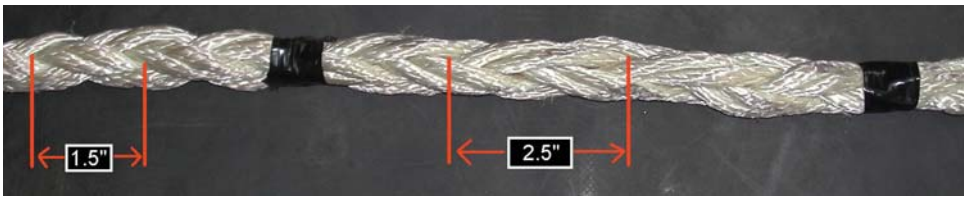

Figure 30: TAO 3/4″ 8-strand plaited nylon: pic length change (E927).

wrapping it around blocks could not cause the change in pik length that was observed. The segments of the nylon line were also pulled to failure, resulting in a 10,300 lb. breaking strength (vs. 15,000 lb. RBS), these numbers are probably not valid, due to the test piece not being long enough (end effects of splices).

The effects of shock loading on the nilspin cable were studied by testing to failure the upper section of nilspin from both KEO deployments. This resulted in an ultimate breaking strength of ∼15,400 lbs. (vs. 13,900 lb. RBS), so there was no strength degradation due to shock loading during deployment.

For future KEO deployments the primary design issue that needs to be

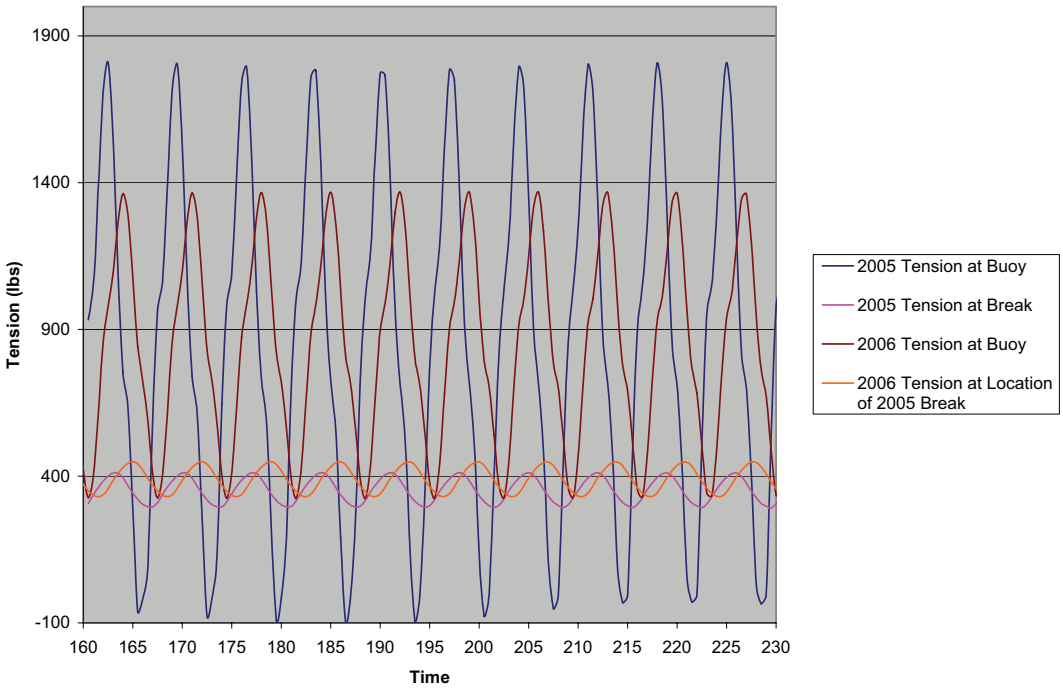

Figure 31: WHOI CABLE dynamic line tension vs. time, 2006 deployment vs. 2005 deployment, instruments modeled as materials for worst case environmental conditions seen at site last year (snapshot 285070000), mean currents, harmonic wave.

addressed is the shock loading of the mooring system. Addressing this design problem, as well as performing a careful physical inspection of the mooring line structure prior to deployment, and tailoring the deployment deck layout to eliminate possible line abrasion, should result in a survivable mooring.

5.2 2006 KEO Mooring Design

In order to alleviate the shock loading on the KEO mooring system, the vertical fall velocity of the inductive cable must be increased. As shown previously (see 3.3, "Shock Loading"), the primary factor impacting the vertical velocity of the inductive cable is the tangential drag on the faired inductive cable, not the vertical drag from the subsurface instruments. Because the currents at the KEO deployment site are in reality much lower than the mooring was initially designed for, fairings can be removed from the inductive cable, decreasing the tangential drag of the cable. After carefully studying the current data for the deployment site (see Fig. 7b), 275 m of fairings were removed from the inductive cable, and the remaining 250 m of fairings were placed, based on the 2005 current profile, between 0–140 m and 240–350 m. WHOI CABLE predicts that the 2006 KEO mooring will survive current conditions up to the maximum currents seen at the site last year +20% (over entire current profile, ∼4 knt surface current, 0.8 knt current to the bottom). The dynamic output of the KEO CABLE mooring model, for both random and harmonic wave states, after the fairings have been re-

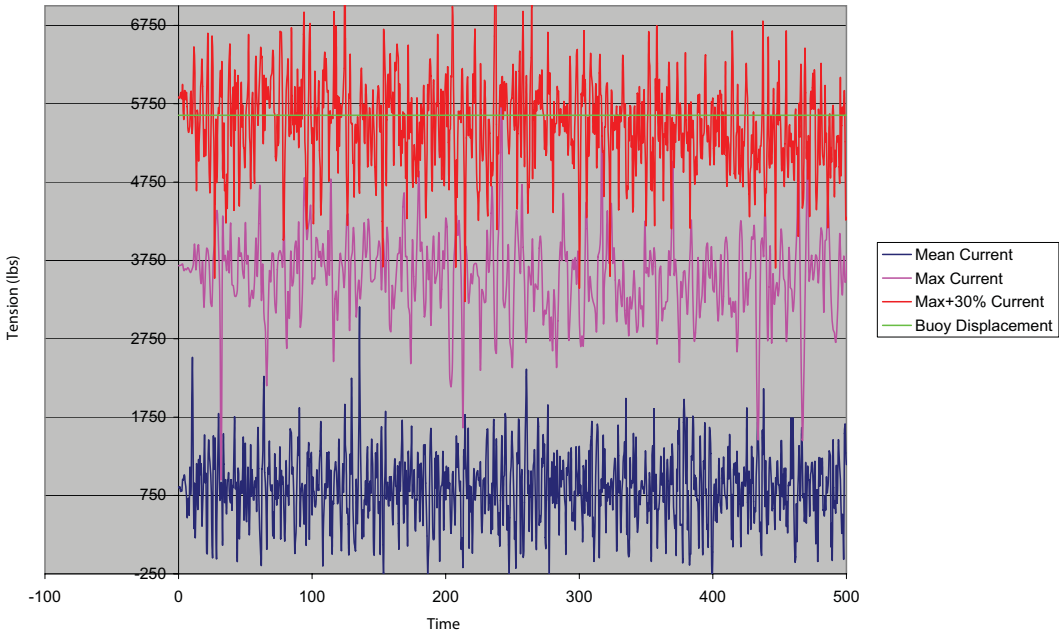

Figure 32: WHOI cable dynamic line tension vs. time, 2006 deployment, instruments modeled as materials for worst case environmental conditions seen at site in 2005, mean currents, max currents, and max currents +30%, random wave.

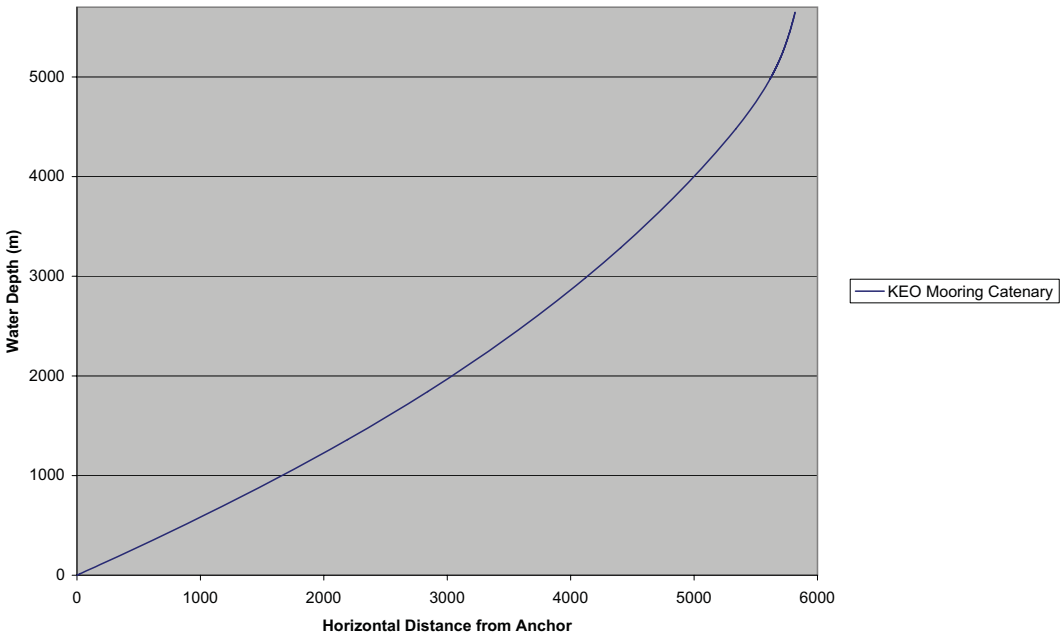

Figure 33: KEO 2006 deployment mooring profile (catenary) during max currents.

moved from the cable, is shown in Figs. 31 and 32. Figure 32 shows that the 2006 mooring might experience shock loading under extreme wave conditions. However, a direct comparison of harmonic wave CABLE output for worst cast shock loading conditions from 2005 to the 2006 model illustrates how removing 275 m of fairings have decreased the overall tension spread, greatly reducing possible instances of shock loading, while maintaining the mean tension from the 2005 deployment (see Fig. 31). Figure 33 shows the 2006 mooring's catenary under maximum current conditions, and the new and improved mooring diagram is shown in Fig. 34.

6. Acknowledgments

The authors would like to thank the following people, for their valuable contributions to this paper: Dr. Meghan Cronin, for her scientific leadership, encouragement, and enthusiasm; Rick Miller, for his mooring expertise and his thorough inspection and analysis of the KEO mooring components; Curran Fey, for his invaluable help in filtering and graphing the various KEO data sets; Ryan Layne Whitney for his help turning this report into a cohesive document; and everybody at PMEL EDD for their comments and suggestions. Thank You!

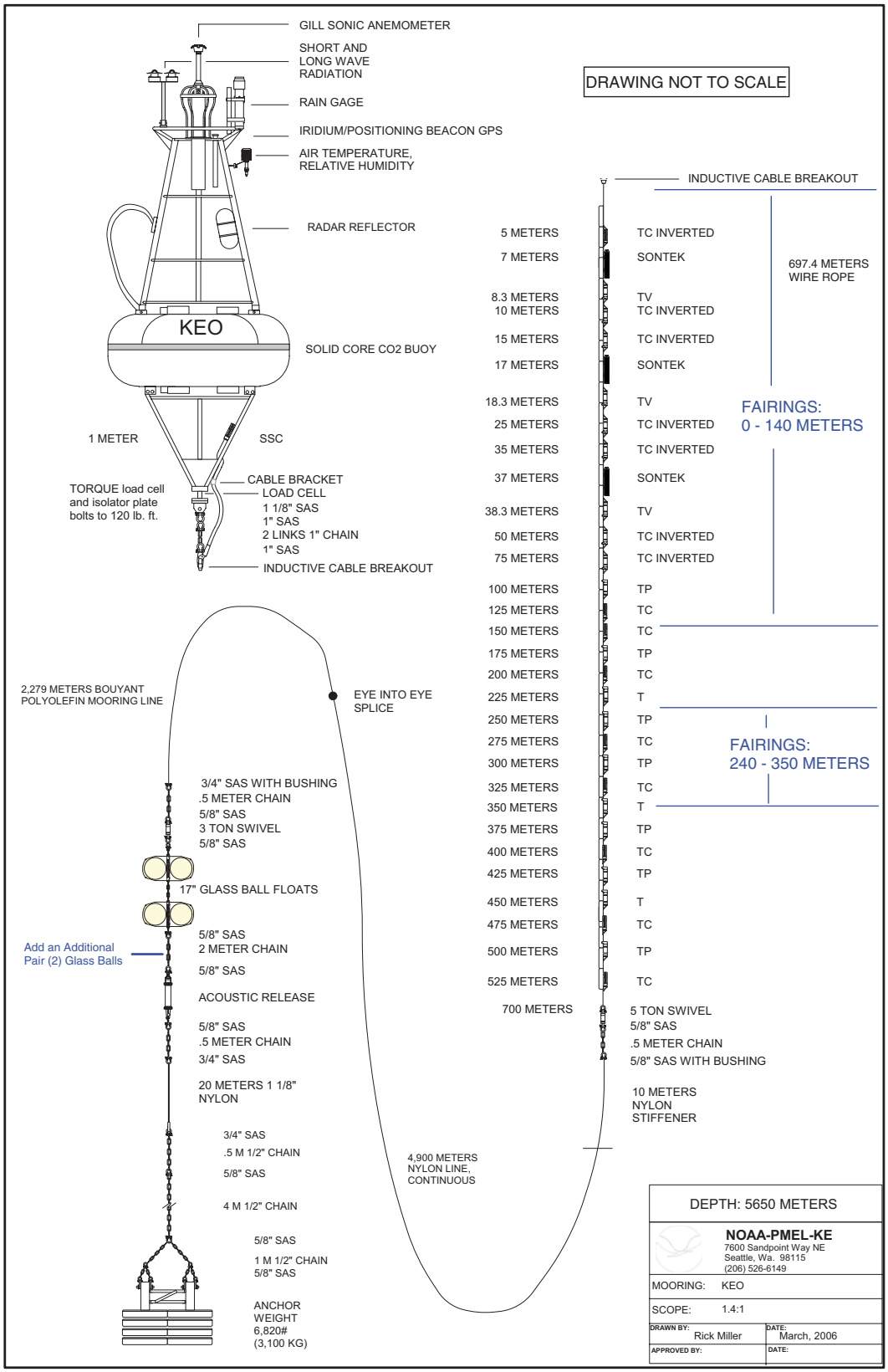

Figure 34: KEO 2006, mooring configuration.